A peer-reviewed version of this preprint was published in PeerJ on 14 June 2019.

View the peer-reviewed version (peerj.com/articles/7121), which is the preferred citable publication unless you specifically need to cite this preprint.

Naqib A, Poggi S, Green SJ. 2019. Deconstructing the Polymerase Chain Reaction II: an improved workflow and effects on artifact formation and primer degeneracy. PeerJ 7:e7121 https://doi.org/10.7717/peerj.7121

PeerJ Preprints NOT PEER-REVIEWED

Deconstructing the Polymerase Chain Reaction II: An improved workflow and effects on artifact formation and primer degeneracy

Ankur Naqib [1, 2] , **Silvana Poggi** [1, 3] , **Stefan J Green** [Corresp. 1]

[1] Sequencing Core, Research Resources Center, University of Illinois at Chicago, Chicago, IL, United States
[2] Rush University, Chicago, IL, United States
[3] Northwestern University, Chicago, IL, United States

Corresponding Author: Stefan J Green
Email address: GreenDNA@uic.edu

Polymerase chain reaction (PCR) amplification of complex microbial genomic DNA templates with degenerate primers can lead to distortion of the underlying community structure due to inefficient primer-template interactions leading to bias. We previously described a method of deconstructed PCR (“PEX PCR”) to separate linear copying and exponential amplification stages of PCR to reduce PCR bias (Green et al. 2015). In this manuscript, we describe an improved deconstructed PCR (“DePCR”) protocol separating linear and exponential stages of PCR and allowing higher throughput of sample processing. We demonstrate that the new protocol shares the same benefits of the original and show that the protocol dramatically and significantly decreases the formation of chimeric sequences during PCR. By employing PCR with annealing temperature gradients, we further show that there is a strong negative correlation between annealing temperature and the evenness of primer utilization in a complex pool of degenerate primers. Shifting primer utilization patterns mirrored shifts in observed microbial community structure in a complex microbial DNA template. We further employed the DePCR method to amplify the same microbial DNA template independently with each primer variant from a degenerate primer pool. The non-degenerate primers generated a broad range of observed microbial communities, but some were highly similar to communities observed with degenerate primer pools. The same experiment conducted with standard PCR led to consistently divergent observed microbial community structure. The DePCR method is simple to perform, is limited to PCR mixes and cleanup steps, and is recommended for reactions in which degenerate primer pools are used or when mismatches between primers and template are possible.

PeerJ Preprints | https://doi.org/10.7287/peerj.preprints.27525v1 | CC BY 4.0 Open Access | rec: 8 Feb 2019, publ: 8 Feb 2019

PeerJ Preprints NOT PEER-REVIEWED

1 **Deconstructing the Polymerase Chain Reaction II: An improved workflow and effects on**
2 **artifact formation and primer degeneracy**

3

4 **Running title: Deconstructed PCR**

5

6 Ankur Naqib[1, 2%], Silvana Poggi[1^], Stefan J. Green*[1]

7 **Author affiliations:** [1]Sequencing Core, Research Resources Center, University of Illinois at
8 Chicago, Chicago, IL**;** [2]Department of Bioengineering, University of Illinois at Chicago,
9 Chicago, Illinois, USA.

10 % Current address: Rush University Medical Center, Chicago, IL

11 ^ Current address: Northwestern University, Chicago, IL

12

13 **Corresponding author:** Stefan J. Green (GreenDNA@uic.edu); 835 S. Wolcott, A-310,
14 Chicago, Illinois, 60612

Abstract

Polymerase chain reaction (PCR) amplification of complex microbial genomic DNA templates with degenerate primers can lead to distortion of the underlying community structure due to inefficient primer-template interactions leading to bias. We previously described a method of deconstructed PCR ("PEX PCR") to separate linear copying and exponential amplification stages of PCR to reduce PCR bias [1]. In this manuscript, we describe an improved deconstructed PCR ("DePCR") protocol separating linear and exponential stages of PCR and allowing higher throughput of sample processing. We demonstrate that the new protocol shares the same benefits of the original and show that the protocol dramatically and significantly decreases the formation of chimeric sequences during PCR. By employing PCR with annealing temperature gradients, we further show that there is a strong negative correlation between annealing temperature and the evenness of primer utilization in a complex pool of degenerate primers. Shifting primer utilization patterns mirrored shifts in observed microbial community structure in a complex microbial DNA template. We further employed the DePCR method to amplify the same microbial DNA template independently with each primer variant from a degenerate primer pool. The non-degenerate primers generated a broad range of observed microbial communities, but some were highly similar to communities observed with degenerate primer pools. The same experiment conducted with standard PCR led to consistently divergent observed microbial community structure. The DePCR method is simple to perform, is limited to PCR mixes and cleanup steps, and is recommended for reactions in which degenerate primer pools are used or when mismatches between primers and template are possible.

36 *Introduction*

37 The small subunit (SSU) ribosomal RNA (rRNA) gene is the most frequently targeted
38 gene in studies of complex microbial systems. A common approach for microbial community
39 studies is to extract genomic DNA (gDNA) from multiple samples, PCR amplify gDNA using
40 locus-specific SSU rRNA gene primers containing sequencing adapters and a sample-specific
41 barcode, and equimolar pooling and sequencing [2]. A number of major caveats are associated
42 with such an approach: (i) Microorganisms contain a variable number of rRNA operons [3, 4]
43 and analyses of rRNA genes present a distorted representation of relative cellular abundance; (ii)
44 PCR primer pools are often degenerate or the primers are anticipated to anneal to template
45 sequences containing mismatches with the primers, thereby producing bias in amplification
46 efficiency among different templates; and (iii) samples are generally heavily amplified (30 cycles
47 or more) leading to the possibility of extensive chimera formation.

48 Recently, we identified a novel source of PCR bias – namely, the simultaneous operation
49 of linear copying and exponential amplification during the early cycles of PCR with degenerate
50 primers [1]. We hypothesized that primer-genomic DNA template annealing operates at a
51 different, and likely lower, efficiency compared to primer-amplicon annealing. These primer-
52 template interactions, operating at different efficiencies, both contribute to distortion of the
53 underlying template community, particularly in the early cycles of PCR. To address this source
54 of bias, we developed the polymerase-exonuclease (PEX) PCR method to separate PCR into two
55 distinct stages of linear copying and exponential amplification. Furthermore, the PEX PCR
56 method prevents the locus-specific primers Although effective, the PEX PCR method requires an
57 enzymatic step (exonuclease), which lengthens the workflow. We sought to improve upon the
58 prior protocol and remove the effort associated with exonuclease treatment. Nonetheless, the

59 PEX PCR method – and the separation of linear copying and exponential amplification – serves
60 as the conceptual foundation for the new method. In PEX PCR, after two cycles of linear
61 amplification with locus-specific primers containing 5' non-degenerate linker sequences, the
62 initial stage of the reaction is terminated, primers are removed with exonuclease I treatment, and
63 the linear copies subsequently amplified using non-degenerate primers targeting the 5' linker
64 sequences **(Figure 1**). Here, we present a method that replaces exonuclease treatment with size-
65 selective bead-based purification (*e.g.* AMPure XP beads) but achieves substantial savings in
66 overall labor and sample manipulation by a pooling of all samples prior to purification.

67 The primary objective of this study was to develop an improved pipeline for utilizing the
68 PEX PCR concept, while retaining the ability to reduce PCR bias. To demonstrate the
69 effectiveness of the updated workflow, we replicated a temperature-gradient analysis of a single
70 complex environmental genomic DNA sample using both standard PCR and DePCR workflows.
71 Data were interrogated to examine the observed microbial community structure by method and
72 reaction annealing temperature. In addition, primer utilization profiles (PUPs) were analyzed to
73 assess the effects of annealing temperature on the relative utilization of each primer within a
74 degenerate pool of primers. Subsequently, we examined the behavior of the amplification system
75 with varying input gDNA. A final experiment examined the ability of each unique primer within
76 a degenerate primer pool to amplify a complex environmental sample using both the standard
77 PCR and DePCR methodologies.

78

79 **Materials and Methods**

80 *DNA Templates*

81 A single microbial genomic DNA (gDNA) sample obtained from chinchilla feces was
82 used for this study. The fecal sample was extracted using the PowerSoil DNA extraction kit (Mo
83 Bio Laboratories, Carlsbad, CA).

84

85 *Primer Synthesis*

86 The primers used for this study are 341F (CCTACGGGAGGCAGCAG) [5, 6] and 806R
87 (GGACTAC**HV**GGGT**W**TCTAAT) [6, 7]. The 806R primer pool is 18-fold degenerate, with
88 theoretical melting temperatures ranging from 54.7°C to 61°C. Melting temperatures of the
89 primers were calculated using the OligoAnalyzer3.1 tool [8], assuming 250 nM primer
90 concentration, 2 mM Mg^{2+}, and 0.2mM dNTPs. Synthesis of the primers was performed either as
91 single degenerate primer pools (standard approach), or as individual primers without
92 degeneracies by Integrated DNA Technologies (IDT; Coralville, IA). Primers were synthesized
93 as LabReady and ordered at a fixed concentration of 100 micromolar. Primers contained
94 common sequence linkers (CS1 and CS2) at the 5' ends, as shown in **Table 1**. Linker sequences
95 are required for the later incorporation of Illumina sequencing adapters and sample-specific
96 barcodes.

97

98 *Standard PCR Protocol*

99 The standard PCR protocol or targeted amplicon sequencing (TAS) protocol is a two-
100 stage NGS library preparation protocol for generating barcoded amplicons ready for Illumina
101 sequencing, and was performed as described previously [9] (**Figure 1A**). Briefly, gDNA was
102 PCR amplified with primers CS1_341F and CS2_806R. The first stage PCR reaction was

103 conducted in a total reaction volume of 10 µl. Each reaction contained 5 µl of MyTaq HS master
104 mix (Bioline, Taunton, MA), 0.5 µl of each primer or degenerate primer at a concentration of 5
105 µM (*e.g.*, CS1_341F and CS2_806R; leading to a 250 nM working concentration), 10 ng of
106 gDNA template, and water up to 10 µl total volume. The first stage of the PCR was conducted
107 using the following thermocycling conditions: 95°C for 5 minutes, followed by 28 cycles of
108 95°C for 30 seconds, annealing temperature (from 40°C to 60°C) for 30 seconds, 72°C for 30
109 seconds; and a final elongation step at 72°C for 7 minutes. Subsequently, a second PCR
110 amplification was performed in 10 µl reactions in 96-well plates to incorporate Illumina
111 sequencing adapters and a sample-specific barcode. A mastermix for the entire plate was made
112 using the MyTaq HS 2X mastermix. Each well received a separate primer pair with a unique 10-
113 base barcode, obtained from the Access Array Barcode Library for Illumina (Fluidigm, South
114 San Francisco, CA; Item# 100-4876). These Access Array primers contained the CS1 and CS2
115 linkers at the 3′ ends of the oligonucleotides. One µl of reaction mixture from the first stage
116 amplification was used as input template for the second stage reaction, without cleanup. Cycling
117 conditions were as follows: 95 °C for 5 minutes, followed by 8 cycles of 95 °C for 30", 60 °C for
118 30" and 72 °C for 30". A final, 7-minute elongation step was performed at 72 °C. Samples were
119 pooled and sequenced on an Illumina MiSeq employing V2 chemistry and 2x250 base reads.

120

121 *Deconstructed PCR (DePCR) Protocol*

122 As with the TAS method, the DePCR method is also a two-stage PCR process (**Figure**
123 **1C)** and is a modification of the previously described PEX PCR method **(Figure 1B)**. For each
124 sample, the first stage reaction was conducted in a 96-well plate with each well containing 5 µl
125 of MyTaq master mix, 0.5 µl of each primer or degenerate primer at a concentration of 5 µM

126 (*e.g.*, CS1_341F and CS2_806R; leading to a 250 nM working concentration), 10 ng of template,
127 1 µl Access Array Barcode Library containing a unique sample-specific barcode, and water up to
128 10 µl. The thermocycler conditions for first stage were composed of two cycles of denaturation
129 at 95°C for 5 minutes and annealing (40°C-60°C, depending on experiment) for 20 minutes,
130 followed by two cycles of denaturation for 5 minutes at 95°C and annealing at 60°C for 20
131 minutes, and a final extension temperature of 72°C for 10 minutes. For temperature gradient
132 experiments, annealing temperatures of 40°C, 45°C, 50°C, 55°C, and 60°C were tested. For
133 single reverse primer variant (RPV) analyses, an annealing temperature of 50°C was used for
134 both TAS and DePCR amplification reactions. Subsequently, a pool composed of 5 µl from the
135 first reaction of each sample was collected and processed for cleanup using AMPure XP beads
136 (Beckman-Coulter) at 0.7X per the manufacturer's recommendations. The cleaning step was
137 performed twice, sequentially. A final elution volume of 20 µl was used to concentrate the
138 sample prior to the second stage of the DePCR reaction. The second stage reactions were
139 conducted in a final volume of 20 µl; the reaction contained 10 µl of MyTaq HS master mix, 1 µl
140 of Illumina P5 (AATGATACGGCGACCACCGA) and P7
141 (CAAGCAGAAGACGGCATACGA) primers, 2 µl of purified template from pooled first stage
142 PCR, and water up to 20 µl. The thermocycler conditions were: 95°C for 3 minutes, 30 cycles at
143 95°C for 15 seconds, 60°C for 30 seconds and 72°C for 30 seconds. Prior to sequencing the pool
144 libraries were purified using a Pippin Prep DNA Size Selection System (Sage Science),
145 employing a 2% agarose gel cassette and selecting for fragment sizes from 450-600 bp.
146 Sequencing of the amplified pool was performed on an Illumina MiSeq employing V2 chemistry
147 and 2x250 base reads. Library preparation and sequencing were performed at the UIC
148 Sequencing Core (UICSQC).

149

150 *Sequence Data Analysis*

151 Raw sequence FASTQ files were merged using the software package PEAR [10], with default
152 parameters. Merged sequences were trimmed using the software package trimmomatic [12].
153 Sequences shorter than 400 bases and longer than 500 bases were removed. Sequences were then
154 screened for chimeras using the USEARCH61 algorithm [11], and putative chimeric sequences
155 were removed from the dataset. Subsequently, sequences were pooled and clustered into
156 operational taxonomic units (OTUs) at a threshold of 97% similarity (QIIME v1.8.0) [13].
157 Representative sequences from all OTUs were annotated using the UCLUST algorithm and the
158 Greengenes 13_8 reference database [14], and a biological observational matrix (BIOM) was
159 generated this annotation pipeline [15]. The BIOM file was analyzed and visualized using the
160 software package Primer7 [16] and the R environment [17]. The R package 'vegan' [18] was
161 employed to generate alpha diversity indices (Shannon, richness, and evenness indices) and to
162 perform rarefaction of BIOM files. Bray-Curtis dissimilarity indices were calculated within the R
163 package 'vegan' and these indices were used to evaluate differences in composition between
164 samples. Analysis of similarity (ANOSIM) calculations were performed at the taxonomic level
165 of genus, using square root transformed data. Initial analysis and processing of the samples was
166 performed using QIIME (v1.8.0) package scripts. Metric multi-dimensional scaling (mMDS)
167 plots were generated using the cmdscale and ggplot2 functions [19] within the R programming
168 environment. Ellipses, representing a 95% confidence interval around group centroids, were
169 drawn assuming a multivariate t-distribution. Some visualizations were performed using the
170 software package OriginPro 2018 (OriginLab, Northampton, Mass).

171

172 *Data Archive*

173 Raw sequence data files were submitted in the Sequence Read Archive (SRA) of the
174 National Center for Biotechnology Information (NCBI). The BioProject identifier of the samples
175 is PRJNA506229. Full metadata for each sample are provided in **Table S1**.

176

177 **Results**

178 *Theory*

179 The Deconstructed PCR (DePCR) method is based on the polymerase-exonuclease (PEX)
180 PCR method described previously [1]. We previously noted that the first two cycles of PCR are
181 unique in that no amplification of the template is performed. Rather, linear copying of the template
182 nucleic acid prepares the reaction for exponential amplification, starting in the third cycle. In the
183 prior manuscript, linear copying of the original gDNA template was separated from exponential
184 amplification of target copies using exonuclease I (**Figure 1B**). Locus-specific primers containing
185 5' linker sequences anneal to genomic DNA during two cycles of amplification. Subsequently,
186 exonuclease I was used to remove unused primers from reaction mixtures. Finally, the copied
187 templates were exponentially amplified using primers targeting the 5' linker sequences but not the
188 source genomic DNA. This approach is viable, but cumbersome due to the need for endonuclease
189 treatment of each sample, and for individual amplification of each sample with primers containing
190 Illumina sequencing adapters and sample-specific barcodes.

191 We modified the original protocol by including both locus-specific primers containing 5'
192 linkers and primers with Illumina sequencing adapters, sample-specific barcodes, and 3' linkers
193 together in the first linear stage of the reaction (**Figure 1C).** Thus, this approach combines primer

194 sets used in both stage A and B of the PEX PCR method in the same reaction. In addition, four
195 cycles of linear copying are performed, instead of two as in the PEX PCR method (**Figures 1 and**
196 **2**). The resulting products are target copies containing Illumina sequencing adapter sequences,
197 sample specific barcodes, linker sequences, and the region of interest. The four cycles of copying
198 serve to prepare the templates for exponential amplification but also (unlike PEX PCR) incorporate
199 a sample-specific barcode so that samples can be pooled and amplified exponentially
200 simultaneously. As with PEX PCR, the linear amplification stage – if operating at 100% efficiency
201 – does not increase the total number of targets from that present in the source template DNA.

202 After linear copying during the first four cycles, the reactions are pooled and purified to remove
203 unincorporated primers. It is essential for the proper functioning of the method that the primers
204 from the initial stage of the reaction are completely removed; otherwise these locus-specific
205 primers continue to interact with template and amplicons during exponential amplification cycles.
206 We observed that a single cleanup using AMPure XP beads (0.7X) was not sufficient to fully
207 remove all primers; therefore, a double cleanup (*i.e.*, two sequential AMPure XP 0.7X cleanups of
208 the pooled reactions) is performed. The final purified DNA includes a range of DNA types, but
209 only the fragments that contain Illumina sequencing adapters at both ends of the molecule have
210 been generated only through linear copying steps and are available for amplification using Illumina
211 P5 and P7 primers (**Figure 2**). The entire pool is then used as input template for subsequent
212 amplification using primers consisting of Illumina P5 and P7 sequences. Linear-copied DNA
213 fragments from all samples within the pool, each now containing a sample-specific barcode, are
214 thus subject to exponential amplification simultaneously. One useful feature of this approach is
215 that hundreds of samples can be amplified simultaneously within a single reaction. The theoretical
216 advantages of this novel workflow include: (1) the elimination of a separate exonuclease step for

217 each sample, (2) the rapid reduction of many reactions into a single reaction for purification and
218 exponential amplification, and (3) all associated benefits of the prior PEX PCR, in which linear
219 and exponential amplification stages of PCR are isolated from each other and where locus-specific
220 primers are only active for two linear cycles of copying.

221

222 *Validation of the DePCR method*

223 To assess the effects of amplification method (TAS vs DePCR) and annealing temperature
224 on observed microbial community structure, a single genomic DNA sample was amplified across
225 multiple annealing temperatures using both amplification strategies. Five technical replicates for
226 each condition were performed, and amplicons were sequenced together. The data were analyzed
227 to determine if there were significant differences in sequence metrics (chimera formation), alpha
228 diversity (richness and Shannon index), and observed community structure (beta diversity analyses
229 performed using multi-dimensional scaling and analysis of similarity (ANOSIM). Rates of
230 detectable chimera formation were several orders of magnitude lower with the DePCR pipeline
231 relative to the TAS pipeline, regardless of annealing temperature (**Table 2**). Average chimera
232 detection rate for TAS-processed samples range from 5.16 to 6.53%, while that for DePCR-
233 processed samples ranged from 0.03-0.1%; this difference was significant at all annealing
234 temperatures tested (ANOVA, $P<0.001$). Low rates of detectable chimeras were found in all
235 experiments conducted with DePCR, with averages in the range of 0.01-0.1% (**Table 2**).
236 Conversely, alpha diversity metrics (genus-level richness and Shannon index), were slightly and
237 significantly higher in TAS-based analyses relative to DePCR. Genus-level richness was on
238 average from 1.06-1.21X higher in TAS analyses relative to DePCR, across annealing
239 temperatures from 40˚C to 60˚C (one-way ANOVA; p values ranged from 1.9E-5 to 1.3E-1; **Table**

240 **3**). Shannon indices were from 1.03-1.06X higher in TAS analyses relative to DePCR across
241 annealing temperatures from 40˚C to 60˚C (ANOVA; p<8.13E-4; **Table 3**).

242 A strong, significant effect of annealing temperature on the observed microbial community
243 structure was seen in both TAS and DePCR amplification methods (**Figure 3A**). Although the
244 overall scale of difference between TAS and DePCR was modest (maximum Bray-Curtis
245 dissimilarity between samples = 0.23 between a TAS sample with 60˚C annealing temperature and
246 a DePCR sample with 40˚C), there was a significant effect of amplification method on observed
247 microbial community at all temperatures. Two-way ANOSIM analyses indicated significant
248 differences by temperature across methods (R=0.832; p=0.0001; **Figure 3B**), and by amplification
249 method across temperatures (R=0.988; p=0.0001; **Figure 3C**). Similar trends were observed for
250 increases in annealing temperature in both methods, with temperature loading primarily on MDS
251 axis 1. As previously noted [1], greater variability in observed microbial community structure was
252 noted with DePCR with low annealing temperature, particularly at 40˚C (**Figure 3A**).

253 One key feature of the DePCR methodology is the ability to determine which primers in a
254 degenerate pool are interacting with the source genomic DNA. This is achieved as the exponential
255 amplification of the template is performed using primers targeting Illumina sequencing adapters
256 and not the locus-specific primers (**Figures 1, 2**). Locus-specific primers only interact with the
257 gDNA and the first linear copies of gDNA during the first two cycles of the DePCR method. These
258 primer sequences are retained during exponential amplification with primers targeting linker
259 sequences. Conversely, in standard PCR, the locus-specific primers interact with both the genomic
260 DNA template and with copies made from the genomic DNA during exponential amplification;
261 thus, information regarding primer-gDNA template interactions are lost [1]. We thus examined the
262 so-called "primer utilization profiles" (PUPs) for these reactions (**Figure 4**). The relative

263 frequency of each of the 18 unique primer variants is shown for each replicate at each PCR
264 condition (temperature x method). Standard PCR amplification protocol (TAS) removes primer-
265 template interaction information as primer-amplicon interactions throughout the amplification
266 reaction tolerate mismatches; all 18 primer variants are used at similar frequencies, regardless of
267 annealing temperature (**Figure 4A**). Some patterning is observed in the TAS method, but overall
268 diversity of primer utilization is extremely high and only small differences were observed between
269 temperatures of 40-60˚C (**Figure 4B**). The average Shannon index for PUP profiles of TAS
270 samples across all annealing temperatures was 2.859-2.864; the maximum possible natural log
271 Shannon index for 18 features is 2.890. This PUP diversity profiling demonstrates that for standard
272 TAS PCR, the primers used in copying throughout the amplification reaction are not dependent on
273 annealing temperature.

274 Conversely, a strong effect of annealing temperature is observed on the PUP of samples
275 amplified using the DePCR protocol (**Figure 4A, B**). A shift in PUP patterning is observed with
276 increasing annealing temperature, and at 60˚C two primer variants (RPV5 and RPV15) dominate.
277 At lower annealing temperatures, a broader range of primers are utilized in the initial stages of
278 gDNA copying. The relationship between annealing temperature and primer utilization richness
279 (here represented as the Shannon index) was best fit with a polynomial equation and is shown in
280 **Figure 4C**. As annealing temperature increases, fewer and fewer primer variants interact with the
281 gDNA template. Conversely, at the lowest tested annealing temperature of 40˚C, the Shannon
282 index of the DePCR amplicons nearly matched that of the TAS. Several primer variants, however,
283 including RPVs 10, 12, 14 and 18, were poorly utilized in DePCR amplifications regardless of
284 annealing temperature (**Figure 4A**). These four variants included variants with high melting
285 temperatures (57.4, 57.5, 58 and 59.8˚C), while the two most utilized RPVs at PCR annealing

286 temperatures of 60˚C had moderate to high annealing temperatures (56.4 and 58.7˚C). Thus, the
287 melting temperature of the primer did not directly correlate with utilization at different PCR
288 annealing temperatures in this system. The observed primer utilization profiles represent a
289 template-specific phenomenon, and different PUPs would be recovered with different DNA
290 templates.

291

292 *Determination of linearity in DePCR amplification*

293 In the DePCR protocol, after four initial cycles of linear copying during the first stage of
294 DePCR, samples are pooled prior to purification and second stage amplification with Illumina P5
295 and P7 primers. The pooling of samples can only be performed because of the incorporation of a
296 sample-specific unique barcode for each sample during the first stage. During the second stage
297 amplification, primers target the Illumina adapters are used for amplification, and all templates
298 from all samples are amplified simultaneously (**Figure 1C**). Since there is no opportunity for
299 primer-template bias during the second stage (*i.e.,* **Stage B of Figure 1C**) of amplification (all
300 amplifiable template molecules contain Illumina sequencing adapters) and primers are non-
301 degenerate, the relative abundance of template molecules from a single sample within the pool
302 should be maintained during amplification. To determine if the relative abundance of template
303 molecules from each sample was maintained in the DePCR protocol, we performed an
304 experiment in which input gDNA (feces) was varied from 1.25 ng to 20 ng per 10 µl reaction.
305 All input levels were performed with five technical replicates. After the first stage (4 cycles) of
306 the DePCR, all replicates from all gDNA input levels were pooled in equal volume and purified.
307 The purified product was then amplified with P5 and P7 primers, and the final pool sequenced.
308 We first assessed whether the input DNA concentration was correlated with the total number of

309 reads generated using this approach (**Figure S1**). Since all samples were amplified together, and
310 low input DNA samples should theoretically provide fewer molecules to the combined pool, we
311 hypothesized that a linear relationship should exist between input DNA in the first stage and the
312 number of reads generated per sample. A significant positive correlation between input gDNA
313 concentration and absolute number of reads recovered from each sample was observed, though
314 substantial variability at each input concentration was observed (R^2=0.58, **Figure S1C**). We also
315 sought to determine if the input gDNA concentration from the same sample had a significant
316 effect on the observed microbial community structure. Although there was a positive correlation
317 between input gDNA and total number of sequences recovered, we observed no significant effect
318 of input gDNA on the microbial community structure (**Figure S1A;** Global ANOSIM R=-0.034;
319 p=0.79**)**. Similarly, no significant difference in primer utilization was observed with different
320 gDNA input concentrations (**Figure S1B**). Thus, increasing input gDNA concentration alters the
321 number of molecules passing to the second stage of the DePCR reaction, but within the observed
322 concentration range does not affect the primer utilization profile or final observed microbial
323 community structure.

324

325 *Assessing the effect of individual primers in a degenerate primer pool*

326 Degenerate primer pools are generally used to amplify genomic DNA, although not all
327 primers actively interact with the source gDNA (**Figure 4A**). This degenerate mixture of primers
328 is employed to target a broad range of taxa , and the presence of additional primer variants in
329 pools has been shown to improve detection of known microbial lineages [21-24]. In standard
330 PCR, all primers do eventually interact with amplified copies of gDNA during the many cycles
331 of exponential amplification; however, many primers do not interact with the source genomic

332 DNA due to preferential annealing of other primers (**Figure 4A**). We sought, therefore, to
333 determine how much microbial diversity could be detected using each primer variant
334 independently in PCR reactions using both the TAS and DePCR methods. In addition, we sought
335 to determine how the observed microbial community structure differed by single primer variant
336 usage. We hypothesized that the single primer variant PCR would better approximate degenerate
337 primer pools when using the DePCR method relative to the TAS method, as our prior work
338 showed that a deconstructed PCR approach was more tolerant of mismatches between primer
339 and gDNA template than TAS [1]. The tolerance of mismatches may lead to better capture of
340 microbial community diversity when a greater number of mismatches between primer and
341 template are present, as is expected in a single primer PCR. To explore this, we PCR-amplified a
342 single gDNA template (feces) with the 18 unique reverse primer variants (RPVs) from the
343 degenerate primer pool. Each reaction was performed in technical duplicates, and each reaction
344 was performed using the DePCR and the TAS method. Three RPVs from the TAS method were
345 removed from the analysis due to pipetting error, as determined by primer utilization profiles.
346 These included one replicate of RPV5 and both replicates of RPV15 (Table S1). We compared
347 alpha and beta diversity analyses of the PCRs employing 15-18 unique RPVs to those generated
348 with the fully degenerate primer set. All alpha and beta diversity analyses were performed on
349 data rarefied to a depth of 1800 sequences/sample (**Table S1 – experiment 3**).

350 When employing fully degenerate primer pools, observed alpha diversity (Shannon
351 index) of the fecal sample was slightly, but significantly higher when analyzed using the TAS
352 protocol relative to the DePCR protocol (average Shannon index, five replicates, 2.71 to 2.66;
353 ANOVA $P<0.001$; **Table 4**). We then calculated average Shannon indices for analyses of the
354 same gDNA sample with individual RPVs, employing TAS and DePCR protocols. The average

355 Shannon index for the TAS reactions with unique RPVs (2.40) was significantly lower than that
356 measured for the DePCR reactions (2.58) (ANOVA P<0.001; **Table 4**). Finally, all RPV data,
357 rarefied to 1800 sequences per sample, was pooled together for TAS and DePCR approaches,
358 independently. These combined datasets were then randomly sub-sampled to 1800 sequences.
359 These rarefactions were performed five times, and the average Shannon index for the combined
360 RPVs was calculated. In this approach, average Shannon index from TAS (2.48) was
361 significantly lower than for DePCR (2.69) (ANOVA P<0.001; **Table 4**). Across all three
362 methods of calculating observed diversity, there was no significant different in measured
363 Shannon index for the DePCR method (ANOVA, P=0.377), while a significant decrease with
364 each RPV independently was observed with the TAS method (ANOVA, P=3.69e-8). When each
365 RPV is used independently in the TAS protocol, the overall captured diversity is lower than with
366 reactions with degenerate pools (**Table 4)** due to the greater number of potential mismatch
367 interactions that can occur when a complex template is amplified with a single, non-degenerate
368 primer. As the DePCR method is more tolerant of mismatches, no significant decrease in average
369 Shannon index was observed. However, the observed variance in Shannon index among the
370 individual RPVs was greater for the DePCR than for the TAS method **(Table 4**).

371 We next examined the structure of the observed fecal microbial communities in standard
372 TAS and DePCR with degenerate primer pools, and with reactions conducted using RPVs
373 (**Figure 5**). We observed high reproducibility for five replicates using TAS (*i.e.*, 'TAS_pool') or
374 DePCR (*i.e.*, 'DePCR_pool') with degenerate primer pools (**Figure 5A, B**) and observed
375 microbial community structure was significantly different between TAS and DePCR employing
376 the degenerate primer pools (ANOSIM, R=0.401, p=0.001). Compared to amplifications with
377 degenerate pools of primers, within-group variability was much greater for the analyses of RPVs

individually with either amplification protocol (**Figure 5A, B, 'TAS' and 'DePCR'**). Within-group Bray-Curtis dissimilarity (BCD) of amplicons from the 15 (TAS) to 18 (DePCR) RPVs ranged from 0.03 to 0.36 for the TAS method and from 0.04 to 0.68 for the DePCR method (ANOVA P<0.001; **Figure 5B**). Conversely, the within-group BCD for five technical replicates generated with degenerate primer pools were 0.04 to 0.07 for TAS and 0.05 to 0.11 for DePCR (ANOVA P<0.001). Profiles of the individual RPVs from DePCR analyses could be divided into two groups: (a) RPVs with profiles highly similar to degenerate primer pool analysis with either DePCR or TAS; and (b) RPVs with profiles divergent from the degenerate pool communities, and more similar to RPVs from TAS amplification reactions. Overall, the observed microbial community structure generated using the DePCR method with RPVs and with degenerate pools was not significantly different (ANOSIM R=-0.306, p=0.99). Conversely, the observed microbial community structure generated using RPVs was significantly different that that observed with degenerate primer pools for the TAS method (ANOSIM R=0.487; p=0.003). Average BCD between TAS_pool and TAS RPV profiles (0.211) was significantly greater than for DePCR_pool and DePCR RPV (0.154) (ANOVA P<0.001; **Figure 5C**). DePCR BCD profiles were heavily weighted toward low dissimilarity, with a long tail of high dissimilarity comparisons. The long tail is a result of some primers generating highly divergent observed microbial communities with the DePCR protocol. Many of the primers which showed the poorest utilization within the degenerate pool (*e.g.*, RPV10, 12, 14, and 18; **node with red dot in Figure 4A**), generated the most divergent single RPV profiles. This suggests that these primers do not closely match the most dominant taxa within this particular gDNA sample.

Discussion

401 We demonstrate here an updated protocol for the Deconstructed PCR methodology [1]
402 which reduces the overall complexity of the workflow and increases the throughput. Complete
403 removal of 1st stage (or "Stage A") primers (locus-specific primers containing 5' overhanging
404 linkers) is essential for the effectiveness of the DePCR protocol, and we have replaced the
405 exonuclease step with a bead-based magnetic cleanup. The new method improves throughput by
406 generating barcoded DNA fragments through 4 cycles of linear amplification; thus, all samples
407 can be pooled before bead-cleanup. This reduces workflow complexity and cost, while retaining
408 the essential features of the DePCR reaction. Complete removal of primers is difficult to measure
409 directly, however; thus, the primer utilization profiles (PUPs) are the clearest indication of
410 successful removal of locus-specific degenerate primers from the first stage of the reaction. With
411 standard PCR, no true signal is obtained from the PUPs, as primer-amplicon interactions during
412 late cycles generates a 'scrambled' signal due to mismatch interaction with amplicons present at
413 high abundance. In DePCR, a PUP signal can be obtained as locus-specific primers only interact
414 with the gDNA template and linear copies during the first two cycles of PCR. Subsequently, all
415 exponential amplification is performed using conserved sequences that are not present in the
416 source gDNA. In this way, the primer sequences interacting with the source gDNA are
417 'fossilized' and can be interrogated directly. When using this approach, we observed strong
418 effects of annealing temperature on primer-gDNA template interactions, with a negative
419 quadratic correlation between annealing temperature and evenness of primer utilization. At
420 highest annealing temperatures, very few primers from the primer pool anneal to the gDNA
421 template, and this leads to a shift in the sequences that are amplified by PCR with a result of
422 significantly different observed microbial communities. We note that the elevated annealing
423 temperature by itself does not select for primer variants with the highest theoretical melting

424 temperature. Rather, primer variants, presumably template-specific, are favored regardless of
425 their melting temperature.

426 A surprising benefit to the DePCR methodology is the reduced rate of chimera
427 formation. Chimeras are artifactual hybrid sequences generated from two or more templates due
428 to incomplete polymerase extension during PCR, and their presence can be difficult to detect and
429 lead to overestimation of diversity and alteration of observed microbial community structure [25-
430 27]. Input genomic DNA concentration and target microbial community complexity have been
431 identified as contributors [28, 29]. We previously observed that chimera formation was
432 correlated with total number of PCR cycles in both first and second stages of PCR [30], and this
433 has been reported elsewhere in many studies [27, 29, 31]. As many factors can contribute to
434 chimera formation, various solutions have been proposed, including reducing input gDNA
435 concentration [32], reducing PCR cycles [20, 33], employing highly processive enzymes [29],
436 among others. In this study, we have observed that the use of the DePCR methodology can
437 dramatically and significantly lower rates of observed chimeras resulting in rates that were
438 generally below 0.1%. These low rates of chimera formation were observed across all annealing
439 temperatures and input template concentrations tested. The reasons for the dramatic decrease in
440 chimera formation rate with the DePCR method are likely a result of: (a) reduction in input DNA
441 concentration for exponential amplification due to the double-purification step, (b) higher
442 annealing temperature for the exponential amplification due to targeting of P5/P7 Illumina
443 adapters –potentially reducing the re-annealing of PCR products to other products, and (c) long
444 elongation times during the first cycles, reducing the formation of incomplete molecules during
445 the first stages of PCR. Conceivably, chimera formation with DePCR could be reduced further;
446 we performed 30 cycles of amplification to generate robust PCR yields for sequencing.

447 However, the amplification of the pool of amplicons during the second stage PCR could be
448 titrated across different numbers of cycles, and the reaction with the fewest numbers of cycles
449 yielding sufficient DNA for sequencing could be employed. It is critical to remember that the
450 rate of chimera formation represents only the rate of *detectable* chimera formation, and that
451 chimeras generated from closely related sequences are not only likely to occur at higher rates
452 [31] but are also essentially undetectable by chimera detection software. We note that in this
453 study, amplification of fecal gDNA with degenerate primer pools resulted in higher observed
454 diversity with the TAS method relative to the same sample amplified with the DePCR protocol
455 (**Table 4**), and this could represent the residual presence of chimeras that were not removed.

456 Suzuki and Giovannoni [20] previously modeled PCR reactions with mixed templates by
457 incorporating efficiency parameters into equations estimating molarity of amplicon yield. They
458 further estimated second-order kinetics wherein changes in the concentration of specific PCR
459 products alter efficiencies during the amplification, including through inhibition of amplification
460 by competition between primers and amplicons for annealing locations. With increasing cycle
461 number, reaction efficiency dropped dramatically. The DePCR method theoretically circumvents
462 at least some of these issues. First, since locus-specific primers interact with template only
463 during two cycles of copying (linear only), any differences in amplification efficiency of
464 templates are limited to those two cycles. Subsequently, all templates are amplified with primers
465 targeting sequences common to all amplifiable templates. Suzuki and Giovannoni [20] showed
466 that even a relatively high amplification efficiency could lead to dramatic distortion of the
467 underlying template ratios within 10-15 cycles. In DePCR approaches, amplification efficiency
468 is expected to be lowest during the first two cycles – when primers anneal to gDNA templates
469 with varying numbers of mismatches – and then higher during the remaining cycles as

470 amplification is performed with perfectly matching primers. We also note that in PCRs with
471 degenerate primers, each primer variant is present at a low concentration (total primer
472 concentration / number of variants); in the 2nd stage of the DePCR protocol, a non-degenerate
473 primer at a high concentration relative to each variant is used for amplification. Thus, DePCR
474 limits the number of cycles operating at low primer efficiency and uses high-efficiency reactions
475 to perform exponential amplification. Degenerate locus-specific primer interactions with PCR
476 amplicons are also removed, thereby removing additional variable efficiency annealing steps
477 from the PCR.

478 We previously demonstrated that a deconstructed PCR approach could help overcome
479 PCR distortions due to mismatches between primers and templates in a mock community [1],
480 and we believe this is in part due to the circumventing of multiple cycles with low amplification
481 efficiency. Single mismatches between templates and primers can substantially alter observed
482 microbial community structure, and indeed, many modifications to degenerate primer pools are
483 performed to increase degeneracy by adding single variants targeting specific microbial taxa
484 [26]. In this study, we independently used each primer variant in a degenerate primer pool both
485 to examine the potential for each primer to amplify a complex microbial gDNA template and to
486 assess the ability of the DePCR protocol to enable single non-degenerate primers to broadly
487 amplify microbial taxa with mismatches. We observed that while the observed microbial
488 community structure varied widely using non-degenerate primer variants (both TAS and
489 DePCR), many single non-degenerate primer variants were able to generate reasonable
490 approximations of the microbial community structure as revealed through amplification reactions
491 with degenerate primer pools, thus indicating that the DePCR approach can be used with
492 complex microbial samples to improve tolerance of mismatches. This suggests that a more

493 empirical approach to primer design can be taken by using the DePCR method to reduce the
494 complexity of degenerate primer pools or enable broader target range of highly degenerate
495 primer pools targeting functional genes. Primer utilization profiling can in turn be used to
496 provide empirical evidence demonstrating which primers within the degenerate primer pool are
497 interacting with unknown templates. The inclusion of non-essential variants decreases the
498 concentration of all other primers in a primer pool, and removal of unneeded primer variants may
499 be beneficial. However, when using the same primer set for a broad range of complex genomic
500 DNA samples from different environments, we expect that the 'essential' primers will vary from
501 system to system.

502 We can recommend the DePCR protocol for reactions where degenerate primer pools are
503 used or for primer-template systems where mismatches are possible or expected. Several caveats,
504 however, should be considered. First, the method is not recommended for reactions requiring
505 stringent PCR conditions. Second, since reactions are pooled together after the first linear cycles
506 and then amplified, the reactions are sensitive to the relative number of copies within each
507 sample. As observed in **Figure S1C**, there is a linear response between input gDNA and number
508 of sequences generated. Thus, input gDNA concentration of similar samples should be carefully
509 controlled to avoid large variance in number of sequences generated per sample. Furthermore,
510 different sample types should be amplified independently, as different samples may have a
511 different density of targets per ng of DNA, leading to further variance in sequence reads
512 generated. Third, in the updated DePCR protocol where Illumina P5 and P7 primer are used,
513 polymerase extension copies through the DNA region containing the sample-specific barcode
514 and can introduce errors. In this study, we employed Fluidigm Access Array primers which
515 contain 10-base barcodes with a Hamming distance of 3 (each barcode has at least 3 mismatches

516 with all other barcodes), and this large Hamming distance should limit mis-assignment of reads.
517 However, with other barcoding systems, or with very high PCR cycle or error-prone
518 polymerases, this source of error could lead to cross-signaling between samples or loss of reads.
519 Finally, we note that when assessing if a DePCR protocol is functioning properly, it is important
520 to employ an analysis of primer utilization across a temperature gradient analysis with standard
521 (TAS) and DePCR workflows. In standard PCR, a small or no effect of temperature should be
522 observed on the PUPs, while a strong shift in primer utilization should be observed with the
523 DePCR protocol. Since primer utilization with DePCR can be extremely broad at low annealing
524 temperatures, it can be difficult to differentiate between a properly operating or failed DePCR
525 protocol without the temperature gradient analysis.

526

527 *Figure Legends*

528 **Figure 1. Schematic of (A) standard (TAS), (B) polymerase-exonuclease (PEX) PCR, and**
529 **(C) Deconstructed PCR (DePCR) workflows.** AT = annealing temperature; ET = Elongation
530 time. CS1 = common sequence 1 adapter. CS2 = common sequence 2 adapter. BC = barcode. FP
531 = Forward primer. RP = Reverse primer. Primer sequences are shown in **Figure 2** and **Table 1**.

532 **Figure 2. Polymerase-generated intermediates in the first stage ("Stage A") of the DePCR**
533 **workflow**.

534 **Figure 3. Effect of PCR methodology and annealing temperature on observed microbial**
535 **communities.** Genus-level abundance data were visualized using metric MDS (mMDS)
536 ordination employing a distance matrix based on Bray-Curtis similarity. For each PCR condition
537 (TAS or DePCR), five technical replicates were analyzed using annealing temperatures of 40°,

538 45°, 50°, 55° or 60° Celsius. Ellipses represent 95% confidence intervals around centroids.
539 Rarefaction was performed to a depth of 4,500 sequences per sample. Observed community
540 structure was significantly different across **(A)** all combinations of temperature and method (one-
541 way ANOSIM Global R=0.713; P=0.0001); **(B)** temperature (two-way ANOSIM R=0.832;
542 p=0.0001), and (**C**) amplification method (two-way ANOSIM R=0.988; P=0.0001).

543 **Figure 4. Effect of annealing temperature and amplification methodology on primer**
544 **utilization profiles (PUPs). (A)** Two-way clustered heatmap of log-transformed primer variant
545 utilization during amplification of fecal genomic DNA. Samples (columns) are color-coded by
546 amplification method (TAS or DePCR) and amplification annealing temperature (40°, 45°, 50°,
547 55° and 60°C), with five technical replicates per condition and rarefaction to 1,800
548 sequences/sample. Primers (rows) are clustered by profile similarity across all samples and
549 represent all 18 primer variants (RPV1 – RPV18) present in the 806R degenerate primer pool.
550 Theoretical melting temperatures for each primer are shown adjacent to primer name. **(B)** mMDS
551 ordination of PUPs based on Bray-Curtis similarity. Vectors represent Pearson correlations
552 (>0.9) for each primer variant. Ellipses represent 95% confidence intervals around centroids for
553 DePCR amplification reactions. Five technical replicates per condition were generated and for
554 each sample, rarefaction was performed to 1,800 sequences. (**C**) Regression analysis was
555 performed was performed on average Shannon index values for primer utilization for each
556 methodology (TAS and DePCR) across annealing temperature. A very small effect of annealing
557 temperature on primer utilization evenness was observed in TAS (orange line). A negative
558 quadratic relationship was observed between annealing temperature and primer utilization
559 evenness in DePCR (blue line). Analyses were based on five technical replicates rarefied to
560 4,500 sequences per sample.

561 **Figure 5. Microbial community structure revealed using individual primer variants with**
562 **TAS and DePCR amplification methodologies.** (**A**) Fecal gDNA was amplified using the 341F
563 primer with18 unique 806R reverse primer variants (RPVs) under standard PCR (TAS) and
564 DePCR workflows. Three RPVs were removed from the TAS analysis due to pipetting error, as
565 described in the text. Genus-level biological observation matrices (BIOMs) were visualized
566 using mMDS. Each amplification with a unique RPV was performed in technical duplicate, and
567 five technical replicates were generated using degenerate primer pools (TAS_pool or
568 DePCR_pool). All samples were rarefied to 1,800 sequences. Ellipses represent 95% confidence
569 intervals around centroids. TAS profiles generated with RPVs were significantly distinct from
570 TAS profiles generated with degenerate primer pools (ANOSIM R=0.487; P=0.003). DePCR
571 profiles generated with RPVs were not significantly distinct from DePCR profiles generated with
572 degenerate primer pools (ANOSIM R=-0.306; P=0.99). **(B)** Within-group Bray-Curtis
573 dissimilarity distributions for profiles generated with RPVs and with degenerate pools. **(C)**
574 Between-group Bray-Curtis dissimilarity distributions for observed microbial community
575 structure generated with RPVs and with degenerate primer pools. Average dissimilarity among
576 TAS_pool and TAS RPV profiles (0.211) was greater than for DePCR_pool and DePCR RPV
577 profiles (0.154) (ANOVA P<0.001).

578 **Figure S1. Effect of input gDNA template concentration on microbial community**
579 **composition and PUPs using DePCR.** Analyses were performed on rarefied data sets (8,000
580 sequences per sample), with five technical replicates for each DNA input level (1.25, 2.5, 5, 10
581 or 20 ng/µl). (**A**) Genus-level mMDS ordination of microbial community structure using a
582 distance matrix based on Bray-Curtis similarity. No significant differences were observed
583 between all the concentrations (Global ANOSIM: R=-0.03376, p=0.79). Ellipses represent a 95%

584 confidence interval around the centroid. (**B**) Primer utilization profiles for all primer variants
585 (RPV1 – RPV18), visualized as a heatmap. (**C**) A positive correlation between input gDNA
586 (1.25, 2.5, 5, 10, 20 ng/µl) and sequence yield was observed. For all input levels, the same
587 gDNA template was used with five technical replicates. All samples were pooled after stage A of
588 DePCR and amplified together using Illumina P5 and P7 primers. Data were rarefied to 8,000
589 sequences per sample.

590

591 *Table Legends*

592 **Table 1. Primers used in this study.**

593 **Table 2. Rates of detectable chimeras in sequence data**. Average rates of detectable chimeras
594 are shown for each experiment performed in this study. Significantly lower rates of chimera
595 formation were observed for DePCR-amplified gDNA samples relative to TAS-amplified
596 samples, across multiple annealing temperatures. No significant difference in chimera formation
597 was observed with DePCR methodology with varying gDNA input levels. Significantly higher
598 chimera formation was also observed with TAS relative to DePCR when individual primer
599 variants (RPVs) were utilized. SD = standard deviation.

600 **Table 3. Alpha diversity indices of observed microbial communities**. Shannon indices were
601 calculated at the taxonomic levels of genus for all samples amplified using TAS and DePCR
602 methodologies across five annealing temperatures of 40°, 45°, 50°, 55° and 60°C. Datasets were
603 rarefied to 4,500 sequences/sample. For each methodology and annealing temperature, an
604 average and standard deviation of five technical replicates is shown. At all temperatures, TAS-

605 amplified samples had higher Shannon indices relative to DePCR-amplified samples. SD =
606 standard deviation.

607 **Table 4. Effects of amplification method and reverse primer variants on observed**
608 **microbial community alpha diversity.** Fecal gDNA was PCR amplified with 18-fold
609 degenerate reverse primer pools (5 technical replicates), and with each unique reverse primer
610 variant (RPV; 2 technical replicates). Data sets were rarefied to 1,800 sequences per sample, and
611 Shannon indices (loge) were calculated. When using fully degenerate primer pools, average
612 Shannon index was significantly higher for TAS methodology relative to DePCR methodology.
613 When data from all reactions with individual RPVs were analyzed, average Shannon index was
614 significantly lower for TAS methodology relative to DePCR methodology. Data from RPVs
615 (1,800 sequences/sample) were pooled and re-rarefied to 1,800 sequences (5 repetitions), and the
616 resulting average Shannon index was significantly lower for the TAS methodology relative to
617 DePCR methodology. Different approaches with the DePCR method did not generate
618 significantly different Shannon indices (ANOVA P=0.377), while the same approaches
619 generated significantly different Shannon indices (ANOVA P<0.001).

620 **Table S1: Mapping file metadata associated with all samples used in this study**

621

622 **References**

623

624 1. Green SJ, Venkatramanan R, Naqib A: **Deconstructing the polymerase chain reaction:**
625 **understanding and correcting bias associated with primer degeneracies and primer-template**
626 **mismatches**. *PloS one* 2015, **10**(5):e0128122.

2. Caporaso JG, Lauber CL, Walters WA, Berg-Lyons D, Huntley J, Fierer N, Owens SM, Betley J, Fraser L, Bauer M: **Ultra-high-throughput microbial community analysis on the Illumina HiSeq and MiSeq platforms**. *The ISME journal* 2012, **6**(8):1621.
3. Klappenbach JA, Saxman PR, Cole JR, Schmidt TM: **rrndb: the ribosomal RNA operon copy number database**. *Nucleic acids research* 2001, **29**(1):181-184.
4. Angly FE, Dennis PG, Skarshewski A, Vanwonterghem I, Hugenholtz P, Tyson GW: **CopyRighter: a rapid tool for improving the accuracy of microbial community profiles through lineage-specific gene copy number correction**. *Microbiome* 2014, **2**(1):11.
5. Muyzer G, De Waal EC, Uitterlinden AG: **Profiling of complex microbial populations by denaturing gradient gel electrophoresis analysis of polymerase chain reaction-amplified genes coding for 16S rRNA**. *Applied environmental microbiology* 1993, **59**(3):695-700.
6. Caporaso JG, Lauber CL, Walters WA, Berg-Lyons D, Lozupone CA, Turnbaugh PJ, Fierer N, Knight R: **Global patterns of 16S rRNA diversity at a depth of millions of sequences per sample**. *Proceedings of the national academy of sciences* 2011, **108**(Supplement 1):4516-4522.
7. Walters W, Hyde ER, Berg-Lyons D, Ackermann G, Humphrey G, Parada A, Gilbert JA, Jansson JK, Caporaso JG, Fuhrman JA: **Improved bacterial 16S rRNA gene (V4 and V4-5) and fungal internal transcribed spacer marker gene primers for microbial community surveys**. *Msystems* 2016, **1**(1):e00009-00015.
8. Owczarzy R, Tataurov AV, Wu Y, Manthey JA, McQuisten KA, Almabrazi HG, Pedersen KF, Lin Y, Garretson J, McEntaggart NO: **IDT SciTools: a suite for analysis and design of nucleic acid oligomers**. *Nucleic acids research* 2008, **36**(suppl_2):W163-W169.
9. Naqib A, Poggi S, Wang W, Hyde M, Kunstman K, Green SJ: **Making and Sequencing Heavily Multiplexed, High-Throughput 16S Ribosomal RNA Gene Amplicon Libraries Using a Flexible, Two-Stage PCR Protocol**. In: *Gene Expression Analysis.* Springer; 2018: 149-169.
10. Zhang J, Kobert K, Flouri T, Stamatakis A: **PEAR: a fast and accurate Illumina Paired-End reAd mergeR**. *Bioinformatics* 2013, **30**(5):614-620.
11. Edgar R: **Usearch**. In.: Lawrence Berkeley National Laboratory (LBNL), Berkeley, CA (United States); 2010.
12. Bolger AM, Lohse M, Usadel B: **Trimmomatic: a flexible trimmer for Illumina sequence data**. *Bioinformatics* 2014, **30**(15):2114-2120.
13. Caporaso JG, Kuczynski J, Stombaugh J, Bittinger K, Bushman FD, Costello EK, Fierer N, Pena AG, Goodrich JK, Gordon JI: **QIIME allows analysis of high-throughput community sequencing data**. *Nature methods* 2010, **7**(5):335.
14. McDonald D, Price MN, Goodrich J, Nawrocki EP, DeSantis TZ, Probst A, Andersen GL, Knight R, Hugenholtz P: **An improved Greengenes taxonomy with explicit ranks for ecological and evolutionary analyses of bacteria and archaea**. *The ISME journal* 2012, **6**(3):610.
15. McDonald D, Clemente JC, Kuczynski J, Rideout JR, Stombaugh J, Wendel D, Wilke A, Huse S, Hufnagle J, Meyer F: **The Biological Observation Matrix (BIOM) format or: how I learned to stop worrying and love the ome-ome**. *GigaScience* 2012, **1**(1):7.
16. Clarke K, Gorley R: **Getting started with PRIMER v7**. *PRIMER-E: Plymouth, Plymouth Marine Laboratory* 2015.
17. Team RC: **R: A language and environment for statistical computing**. 2013.
18. Oksanen J, Blanchet FG, Kindt R, Legendre P, Minchin PR, O'hara R, Simpson GL, Solymos P, Stevens MHH, Wagner H: **vegan: Community ecology package**. *R package version* 2011:117-118.
19. Wickham HJJSS: **ggplot2: elegant graphics for data analysis**. 2010, **35**(1):65-88.
20. Suzuki MT, Giovannoni SJ: **Bias caused by template annealing in the amplification of mixtures of 16S rRNA genes by PCR**. *Applied environmental microbiology* 1996, **62**(2):625-630.

675 21. Hayashi H, Sakamoto M, Benno Y: **Evaluation of three different forward primers by terminal**
676 **restriction fragment length polymorphism analysis for determination of fecal Bifidobacterium**
677 **spp. in healthy subjects**. *Microbiology and immunology* 2004, **48**(1):1-6.

678 22. Frank JA, Reich CI, Sharma S, Weisbaum JS, Wilson BA, Olsen GJ: **Critical evaluation of two**
679 **primers commonly used for amplification of bacterial 16S rRNA genes**. *Applied environmental*
680 *microbiology* 2008, **74**(8):2461-2470.
681 23. Parada AE, Needham DM, Fuhrman JA: **Every base matters: assessing small subunit rRNA**
682 **primers for marine microbiomes with mock communities, time series and global field samples**.
683 *Environmental microbiology* 2016, **18**(5):1403-1414.
684 24. Apprill A, McNally S, Parsons R, Weber L: **Minor revision to V4 region SSU rRNA 806R gene**
685 **primer greatly increases detection of SAR11 bacterioplankton**. *Aquatic Microbial Ecology* 2015,
686 **75**(2):129-137.
687 25. Hugenholtz P, Huber T: **Chimeric 16S rDNA sequences of diverse origin are accumulating in the**
688 **public databases**. *International journal of systematic and evolutionary microbiology* 2003,
689 **53**(1):289-293.
690 26. Schloss PD, Gevers D, Westcott SL: **Reducing the effects of PCR amplification and sequencing**
691 **artifacts on 16S rRNA-based studies**. *PloS one* 2011, **6**(12):e27310.
692 27. Edgar RC, Haas BJ, Clemente JC, Quince C, Knight R: **UCHIME improves sensitivity and speed of**
693 **chimera detection**. *Bioinformatics* 2011, **27**(16):2194-2200.
694 28. Fonseca V, Nichols B, Lallias D, Quince C, Carvalho G, Power D, Creer S: **Sample richness and**
695 **genetic diversity as drivers of chimera formation in nSSU metagenetic analyses**. *Nucleic Acids*
696 *Research* 2012, **40**(9):e66-e66.
697 29. Lahr DJ, Katz LA: **Reducing the impact of PCR-mediated recombination in molecular evolution**
698 **and environmental studies using a new-generation high-fidelity DNA polymerase**.
699 *Biotechniques* 2009, **47**(4):857-866.
700 30. Ionescu D, Overholt WA, Lynch MD, Neufeld JD, Naqib A, Green SJ: **Microbial community**
701 **analysis using high-throughput amplicon sequencing**. In: *Manual of Environmental*
702 *Microbiology, Fourth Edition.* American Society of Microbiology; 2016: 2.4. 2-1-2.4. 2-26.
703 31. Wang GC, Wang Y: **The frequency of chimeric molecules as a consequence of PCR co-**
704 **amplification of 16S rRNA genes from different bacterial species**. *Microbiology* 1996,
705 **142**(5):1107-1114.
706 32. D'Amore R, Ijaz UZ, Schirmer M, Kenny JG, Gregory R, Darby AC, Shakya M, Podar M, Quince C,
707 Hall N: **A comprehensive benchmarking study of protocols and sequencing platforms for 16S**
708 **rRNA community profiling**. *BMC genomics* 2016, **17**(1):55.
709 33. Kanagawa T: **Bias and artifacts in multitemplate polymerase chain reactions (PCR)**. *Journal of*
710 *bioscience and bioengineering* 2003, **96**(4):317-323.

711

Figure 1(on next page)

Schematic of (A) standard (TAS), (B) polymerase-exonuclease (PEX) PCR, and (C) Deconstructed PCR (DePCR) workflows.

AT = annealing temperature; ET = Elongation time. CS1 = common sequence 1 adapter. CS2 = common sequence 2 adapter. BC = barcode. FP = Forward primer. RP = Reverse primer. Primer sequences are shown in **Figure 2** and **Table 1**.

PeerJ Preprints NOT PEER-REVIEWED

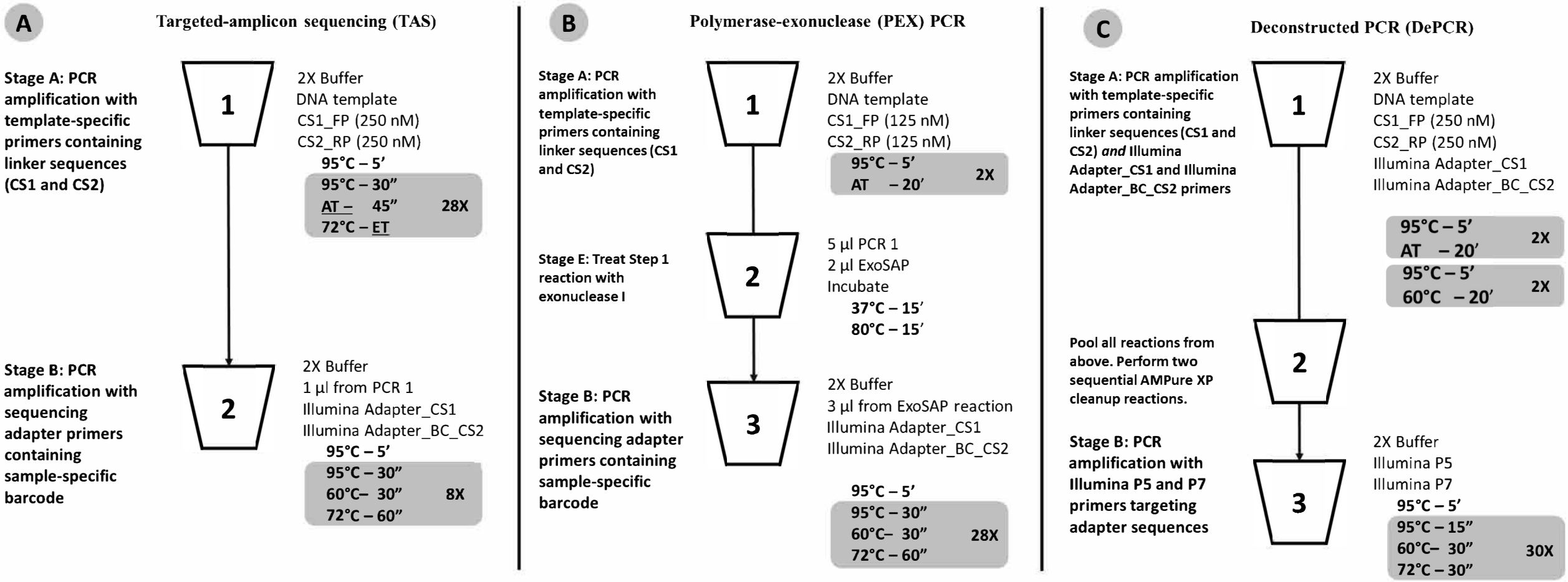

PeerJ Preprints | https://doi.org/10.7287/peerj.preprints.27525v1 | CC BY 4.0 Open Access | rec: 8 Feb 2019, publ: 8 Feb 2019

Figure 2(on next page)

Polymerase-generated intermediates in the first stage ("Stage A") of the DePCR workflow.

Peer Preprints NOT PEER-REVIEWED

CS1_341F 5′-ACACTGACGACATGGTTCTACACCTACGGGAGGCAGCAG-3′
CS2_806R 5′-TACGGTAGCAGAGACTTGGTCTGGACTACHVGGGTWTCTAAT-3′
PE1-CS1 5′-AATGATACGGCGACCACCGAGATCTACACTGACGACATGGTTCTACA-3′
PE2-[BC]-CS2 5′-CAAGCAGAAGACGGCATACGAGATXXXXXXXXXXTACGGTAGCAGAGACTTGGTCT-3′
P5 5′-AATGATACGGCGACCACCGA-3′
P7 5′-CAAGCAGAAGACGGCATACGA-3′

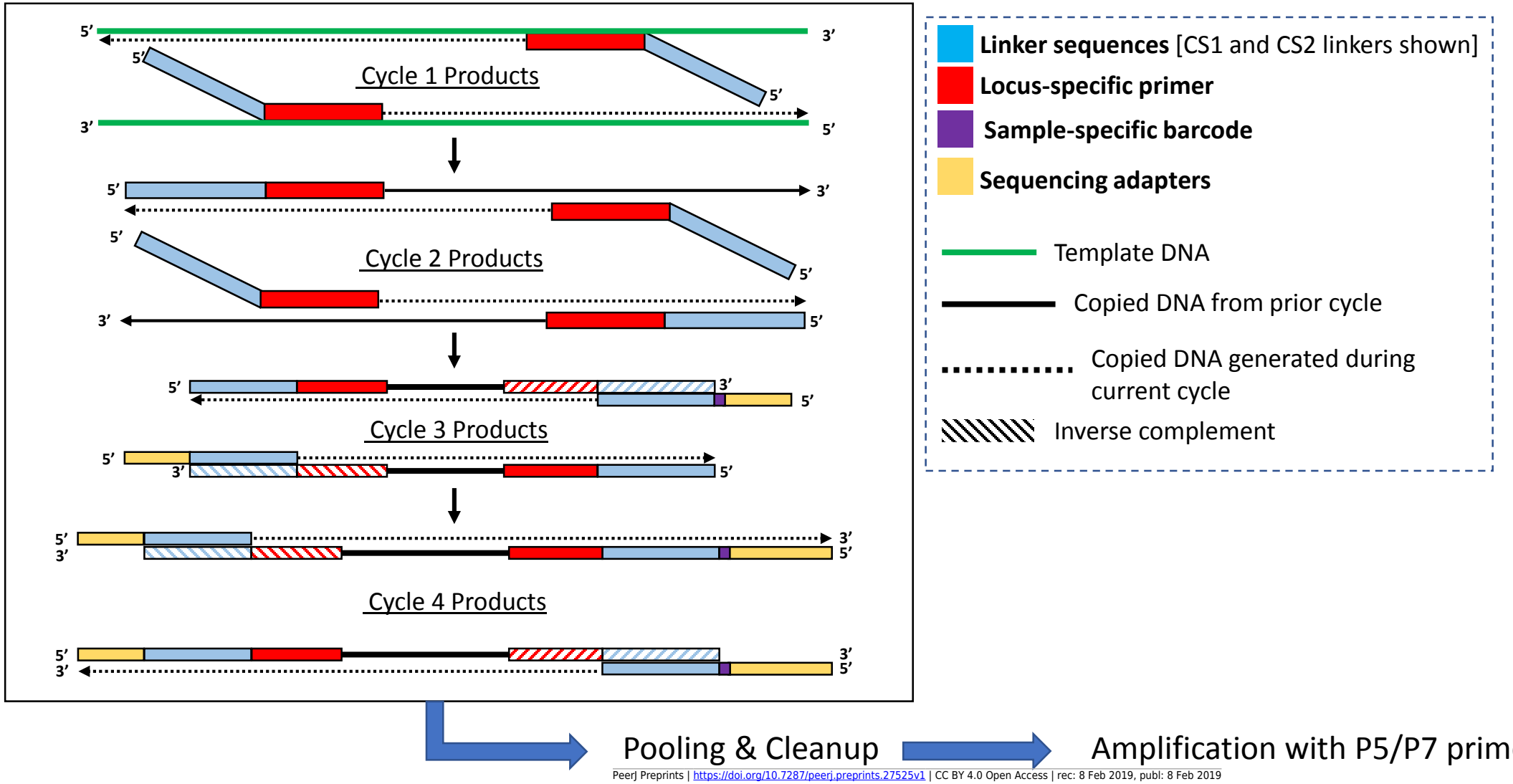

PeerJ Preprints | https://doi.org/10.7287/peerj.preprints.27525v1 | CC BY 4.0 Open Access | rec: 8 Feb 2019, publ: 8 Feb 2019

Figure 3(on next page)

Effect of PCR methodology and annealing temperature on observed microbial communities.

Genus-level abundance data were visualized using metric MDS (mMDS) ordination employing a distance matrix based on Bray-Curtis similarity. For each PCR condition (TAS or DePCR), five technical replicates were analyzed using annealing temperatures of 40°, 45°, 50°, 55° or 60° Celsius. Ellipses represent 95% confidence intervals around centroids. Rarefaction was performed to a depth of 4,500 sequences per sample. Observed community structure was significantly different across **(A)** all combinations of temperature and method (one-way ANOSIM Global R=0.713; P=0.0001); **(B)** temperature (two-way ANOSIM R=0.832; p=0.0001), and (**C**) amplification method (two-way ANOSIM R=0.988; P=0.0001).

PeerJ Preprints
NOT PEER-REVIEWED

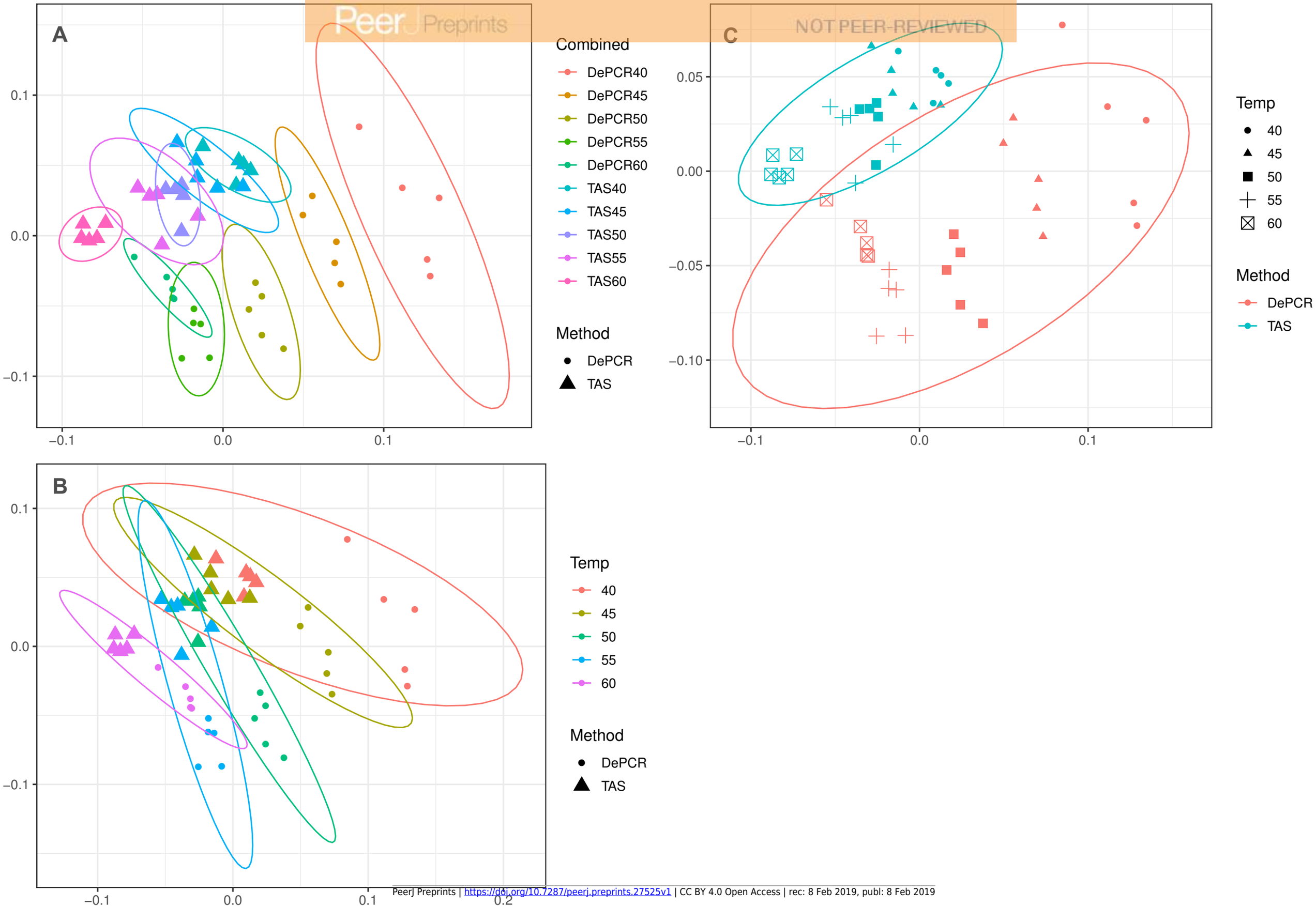

PeerJ Preprints | https://doi.org/10.7287/peerj.preprints.27525v1 | CC BY 4.0 Open Access | rec: 8 Feb 2019, publ: 8 Feb 2019

Figure 4(on next page)

Effect of annealing temperature and amplification methodology on primer utilization profiles (PUPs).

(A) Two-way clustered heatmap of log-transformed primer variant utilization during amplification of fecal genomic DNA. Samples (columns) are color-coded by amplification method (TAS or DePCR) and amplification annealing temperature (40°, 45°, 50°, 55° and 60°C), with five technical replicates per condition and rarefaction to 1,800 sequences/sample. Primers (rows) are clustered by profile similarity across all samples and represent all 18 primer variants (RPV1 – RPV18) present in the 806R degenerate primer pool. Theoretical melting temperatures for each primer are shown adjacent to primer name. **(B)** mMDS ordination of PUPs based on Bray-Curtis similarity. Vectors represent Pearson correlations (>0.9) for each primer variant. Ellipses represent 95% confidence intervals around centroids for DePCR amplification reactions. Five technical replicates per condition were generated and for each sample, rarefaction was performed to 1,800 sequences. (**C**) Regression analysis was performed was performed on average Shannon index values for primer utilization for each methodology (TAS and DePCR) across annealing temperature. A very small effect of annealing temperature on primer utilization evenness was observed in TAS (orange line). A negative quadratic relationship was observed between annealing temperature and primer utilization evenness in DePCR (blue line). Analyses were based on five technical replicates rarefied to 4,500 sequences per sample.

PeerJ Preprints NOT PEER-REVIEWED

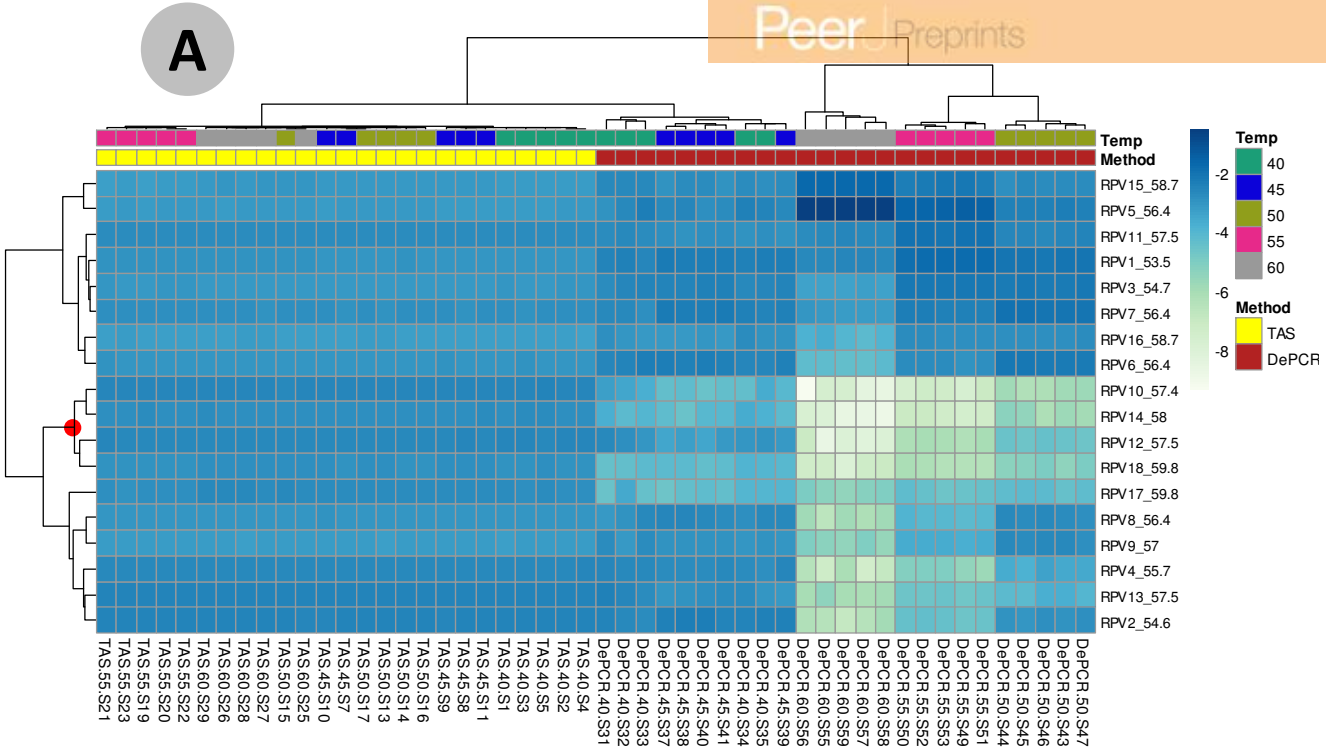

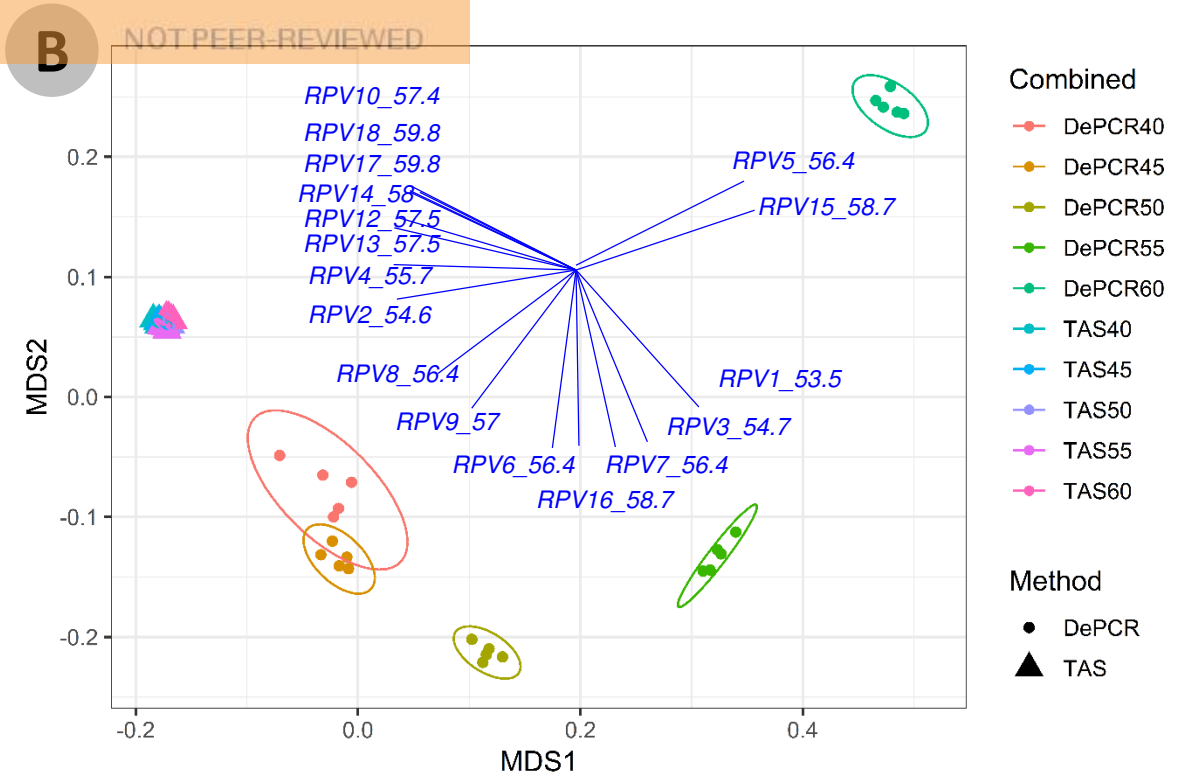

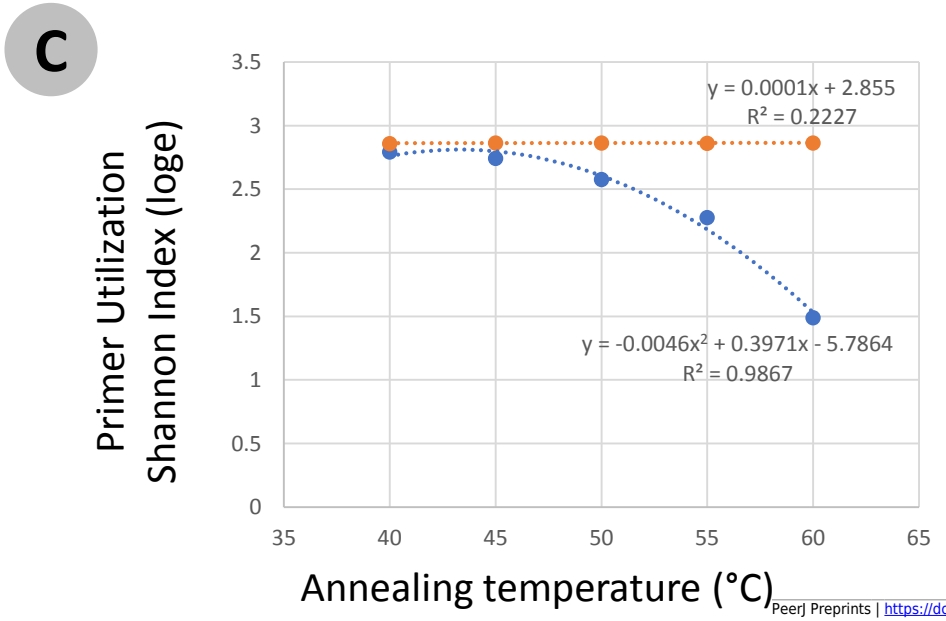

PeerJ Preprints | https://doi.org/10.7287/peerj.preprints.27525v1 | CC BY 4.0 Open Access | rec: 8 Feb 2019, publ: 8 Feb 2019

Figure 5(on next page)

Microbial community structure revealed using individual primer variants with TAS and DePCR amplification methodologies.

(**A**) Fecal gDNA was amplified using the 341F primer with18 unique 806R reverse primer variants (RPVs) under standard PCR (TAS) and DePCR workflows. Three RPVs were removed from the TAS analysis due to pipetting error, as described in the text. Genus-level biological observation matrices (BIOMs) were visualized using mMDS. Each amplification with a unique RPV was performed in technical duplicate, and five technical replicates were generated using degenerate primer pools (TAS_pool or DePCR_pool). All samples were rarefied to 1,800 sequences. Ellipses represent 95% confidence intervals around centroids. TAS profiles generated with RPVs were significantly distinct from TAS profiles generated with degenerate primer pools (ANOSIM R=0.487; P=0.003). DePCR profiles generated with RPVs were not significantly distinct from DePCR profiles generated with degenerate primer pools (ANOSIM R=-0.306; P=0.99). **(B)** Within-group Bray-Curtis dissimilarity distributions for profiles generated with RPVs and with degenerate pools. **(C)** Between-group Bray-Curtis dissimilarity distributions for observed microbial community structure generated with RPVs and with degenerate primer pools. Average dissimilarity among TAS_pool and TAS RPV profiles (0.211) was greater than for DePCR_pool and DePCR RPV profiles (0.154) (ANOVA P<0.001).

PeerJ Preprints NOT PEER-REVIEWED

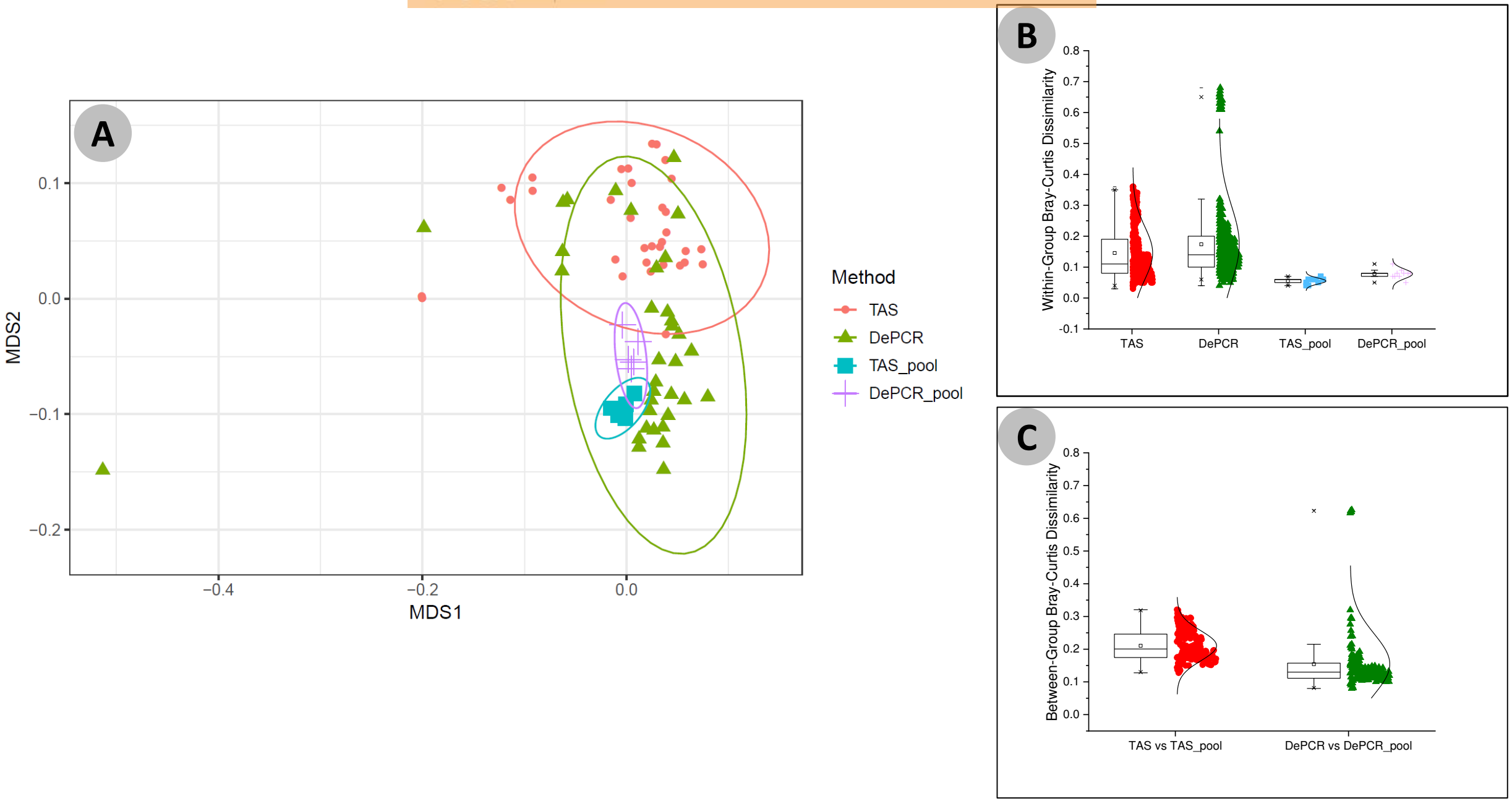

PeerJ Preprints | https://doi.org/10.7287/peerj.preprints.27525v1 | CC BY 4.0 Open Access | rec: 8 Feb 2019, publ: 8 Feb 2019

PeerJ Preprints NOT PEER-REVIEWED

Table 1 (on next page)

Primers used in this study.

PeerJ Preprints NOT PEER-REVIEWED

341F Primer	Primer Sequence	Linker (CS1) Sequence	Final Sequence Name	Final Sequence Ordered
341F	CCTACGGGAGGCAGCAG	**ACACTGACGACATGGTTCTACA**	>CS1_515F	**ACACTGACGACATGGTTCTACA**CCTACGGGAGGCAGCAG

806R Primer and Variants	Primer Sequence	Linker (CS2) Sequence	Final Sequence Name	Final Sequence Ordered
806R	GGACTACHVGGGTWTCTAAT	**TACGGTAGCAGAGACTTGGTCT**	>CS2_806R	**TACGGTAGCAGAGACTTGGTCT**GGACTACHVGGGTWTCTAAT
806R-RPV1	GGACTACTAGGGTATCTAAT	**TACGGTAGCAGAGACTTGGTCT**	>CS2_806R_V1	**TACGGTAGCAGAGACTTGGTCT**GGACTACTAGGGTATCTAAT
806R-RPV2	GGACTACTAGGGTTTCTAAT	**TACGGTAGCAGAGACTTGGTCT**	>CS2_806R_V2	**TACGGTAGCAGAGACTTGGTCT**GGACTACTAGGGTTTCTAAT
806R-RPV3	GGACTACAAGGGTATCTAAT	**TACGGTAGCAGAGACTTGGTCT**	>CS2_806R_V3	**TACGGTAGCAGAGACTTGGTCT**GGACTACAAGGGTATCTAAT
806R-RPV4	GGACTACAAGGGTTTCTAAT	**TACGGTAGCAGAGACTTGGTCT**	>CS2_806R_V4	**TACGGTAGCAGAGACTTGGTCT**GGACTACAAGGGTTTCTAAT
806R-RPV5	GGACTACCAGGGTATCTAAT	**TACGGTAGCAGAGACTTGGTCT**	>CS2_806R_V5	**TACGGTAGCAGAGACTTGGTCT**GGACTACCAGGGTATCTAAT
806R-RPV6	GGACTACAGGGGTATCTAAT	**TACGGTAGCAGAGACTTGGTCT**	>CS2_806R_V6	**TACGGTAGCAGAGACTTGGTCT**GGACTACAGGGGTATCTAAT
806R-RPV7	GGACTACTGGGGTATCTAAT	**TACGGTAGCAGAGACTTGGTCT**	>CS2_806R_V7	**TACGGTAGCAGAGACTTGGTCT**GGACTACTGGGGTATCTAAT
806R-RPV8	GGACTACTCGGGTATCTAAT	**TACGGTAGCAGAGACTTGGTCT**	>CS2_806R_V8	**TACGGTAGCAGAGACTTGGTCT**GGACTACTCGGGTATCTAAT
806R-RPV9	GGACTACACGGGTATCTAAT	**TACGGTAGCAGAGACTTGGTCT**	>CS2_806R_V9	**TACGGTAGCAGAGACTTGGTCT**GGACTACACGGGTATCTAAT
806R-RPV10	GGACTACTCGGGTTTCTAAT	**TACGGTAGCAGAGACTTGGTCT**	>CS2_806R_V10	**TACGGTAGCAGAGACTTGGTCT**GGACTACTCGGGTTTCTAAT
806R-RPV11	GGACTACCAGGGTTTCTAAT	**TACGGTAGCAGAGACTTGGTCT**	>CS2_806R_V11	**TACGGTAGCAGAGACTTGGTCT**GGACTACCAGGGTTTCTAAT
806R-RPV12	GGACTACAGGGGTTTCTAAT	**TACGGTAGCAGAGACTTGGTCT**	>CS2_806R_V12	**TACGGTAGCAGAGACTTGGTCT**GGACTACAGGGGTTTCTAAT
806R-RPV13	GGACTACTGGGGTTTCTAAT	**TACGGTAGCAGAGACTTGGTCT**	>CS2_806R_V13	**TACGGTAGCAGAGACTTGGTCT**GGACTACTGGGGTTTCTAAT
806R-RPV14	GGACTACACGGGTTTCTAAT	**TACGGTAGCAGAGACTTGGTCT**	>CS2_806R_V14	**TACGGTAGCAGAGACTTGGTCT**GGACTACACGGGTTTCTAAT
806R-RPV15	GGACTACCGGGGTATCTAAT	**TACGGTAGCAGAGACTTGGTCT**	>CS2_806R_V15	**TACGGTAGCAGAGACTTGGTCT**GGACTACCGGGGTATCTAAT
806R-RPV16	GGACTACCCGGGTATCTAAT	**TACGGTAGCAGAGACTTGGTCT**	>CS2_806R_V16	**TACGGTAGCAGAGACTTGGTCT**GGACTACCCGGGTATCTAAT
806R-RPV17	GGACTACCGGGGTTTCTAAT	**TACGGTAGCAGAGACTTGGTCT**	>CS2_806R_V17	**TACGGTAGCAGAGACTTGGTCT**GGACTACCGGGGTTTCTAAT
806R-RPV18	GGACTACCCGGGTTTCTAAT	**TACGGTAGCAGAGACTTGGTCT**	>CS2_806R_V18	**TACGGTAGCAGAGACTTGGTCT**GGACTACCCGGGTTTCTAAT

Illumina Primers				Final Sequence Ordered
P5				AATGATACGGCGACCACCGA
P7				CAAGCAGAAGACGGCATACGA

1

Table 2 (on next page)

Rates of detectable chimeras in sequence data.

Average rates of detectable chimeras are shown for each experiment performed in this study. Significantly lower rates of chimera formation were observed for DePCR-amplified gDNA samples relative to TAS-amplified samples, across multiple annealing temperatures. No significant difference in chimera formation was observed with DePCR methodology with varying gDNA input levels. Significantly higher chimera formation was also observed with TAS relative to DePCR when individual primer variants (RPVs) were utilized. SD = standard deviation.

Experiment	PCR Method	Annealing Temp. (°C)	Input concentration (ng/reaction)	Chimera detection rate [Average (SD)]	ANOVA
Annealing temperature	TAS	40	10	5.16% (0.37%)	1.41E-09
	DePCR	40	10	0.05% (0.03%)	
	TAS	45	10	6.49% (0.29%)	4.05E-11
	DePCR	45	10	0.10% (0.07%)	
	TAS	50	10	6.53% (0.21%)	2.02E-12
	DePCR	50	10	0.04% (0.02%)	
	TAS	55	10	5.69% (0.39%)	9.66E-10
	DePCR	55	10	0.05% (0.02%)	
	TAS	60	10	5.46% (0.49%)	7.56E-09
	DePCR	60	10	0.03% (0.02%)	
Input gDNA concentration	DePCR	50	20	0.05% (0.02%)	5.20E-01
	DePCR	50	10	0.03% (0.03%)	
	DePCR	50	5	0.03% (0.01%)	
	DePCR	50	2.5	0.02% (0.01%)	
	DePCR	50	1.25	0.03% (0.03%)	
Reverse primer variants	TAS	50	10	11.98% (3.85%)	0.00
	DePCR	50	10	0.06% (0.08%)	

1

Table 3 (on next page)

Alpha diversity indices of observed microbial communities.

Shannon indices were calculated at the taxonomic levels of genus for all samples amplified using TAS and DePCR methodologies across five annealing temperatures of 40°, 45°, 50°, 55° and 60°C. Datasets were rarefied to 4,500 sequences/sample. For each methodology and annealing temperature, an average and standard deviation of five technical replicates is shown. At all temperatures, TAS-amplified samples had higher Shannon indices relative to DePCR-amplified samples. SD = standard deviation.

PCR Method	Annealing Temp. (°C)	Shannon Index [Average (SD)]	ANOVA	Richness [Average (SD)]	ANOVA
TAS	40	2.69 (0.02)	4.76E-05	61.20 (1.92)	1.92E-05
DePCR	40	2.55 (0.03)		50.60 (1.82)	
TAS	45	2.72 (0.03)	5.86E-05	60.60 (2.70)	1.32E-01
DePCR	45	2.59 (0.03)		57.20 (3.63)	
TAS	50	2.74 (0.03)	2.58E-04	64.00 (2.65)	6.56E-02
DePCR	50	2.66 (0.01)		59.60 (3.78)	
TAS	55	2.72 (0.02)	8.13E-04	62.00 (1.87)	2.98E-02
DePCR	55	2.64 (0.03)		58.60 (2.19)	
TAS	60	2.72 (0.01)	6.16E-04	60.60 (2.70)	3.31E-02
DePCR	60	2.63 (0.03)		56.60 (2.19)	

Table 4(on next page)

Effects of amplification method and reverse primer variants on observed microbial community alpha diversity.

Fecal gDNA was PCR amplified with 18-fold degenerate reverse primer pools (5 technical replicates), and with each unique reverse primer variant (RPV; 2 technical replicates). Data sets were rarefied to 1,800 sequences per sample, and Shannon indices (loge) were calculated. When using fully degenerate primer pools, average Shannon index was significantly higher for TAS methodology relative to DePCR methodology. When data from all reactions with individual RPVs were analyzed, average Shannon index was significantly lower for TAS methodology relative to DePCR methodology. Data from RPVs (1,800 sequences/sample) were pooled and re-rarefied to 1,800 sequences (5 repetitions), and the resulting average Shannon index was significantly lower for the TAS methodology relative to DePCR methodology. Different approaches with the DePCR method did not generate significantly different Shannon indices (ANOVA $P=0.377$), while the same approaches generated significantly different Shannon indices (ANOVA $P<0.001$).

PeerJ Preprints NOT PEER-REVIEWED

Comparison	# replicates analyzed	Average Shannon Index (SD), TAS	Average Shannon Index (SD), DePCR	ANOVA
Amplification with 18-fold degenerate primer pools	5	2.71 (0.03)	2.66 (0.04)	3.14E-05
Amplification with each RPV independently	33 (TAS) or 36 (DePCR)	2.4 (0.01)	2.58 (0.21)	5.95E-05
Summation of independent RPVs and re-rarefaction to 1800 sequences (5x)	5	2.48 (0.03)	2.69 (0.02)	7.40E-07
	ANOVA	3.69E-08	3.77E-01	

1

PeerJ Preprints | https://doi.org/10.7287/peerj.preprints.27525v1 | CC BY 4.0 Open Access | rec: 8 Feb 2019, publ: 8 Feb 2019